

Effect of Iodine Addition on Solid-State Electrolyte LiI/3-Hydroxypropionitrile (1:4) for Dye-Sensitized Solar Cells

Hongxia Wang, Xizhe Liu, Zhaoxiang Wang, Hong Li, Dongmei Li, Qingbo Meng,* and Liquan Chen

Beijing National Laboratory for Condensed Matter Physics, Institute of Physics, Chinese Academy of Sciences, Beijing 100080, China

Received: December 7, 2005; In Final Form: February 7, 2006

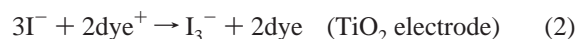
It was observed that the ionic conductivity of the solid-state electrolyte LiI/3-hydroxypropionitrile (HPN) = 1:4 (molar ratio) decreased dramatically with increasing iodine (I_2) concentration, which differs from the conduction behavior of the Grotthuss transport mechanism observed in liquid or gel electrolytes. The short-circuit photocurrent density (J_{sc}) of the dye-sensitized solar cell (DSSC) based on this electrolyte system increases with increasing I_2 concentration until LiI/ I_2 is 1:0.05 (molar ratio). Beyond this limitation, the J_{sc} decreases. At low I_2 concentrations ($I_2/LiI \leq 0.05$), the J_{sc} is mainly affected by the diffusion of I_3^- . An increase of the I_2 concentration leads to the enhancement of the diffusion of I_3^- and an increase of the J_{sc} . At high I_2 concentrations ($I_2/LiI > 0.05$), the factors, including the increased light absorption by the I_3^- , the increased recombination of electrons at the photoanode with I_3^- , and the reduced ionic conductivity of the electrolyte, lead to a decrease of J_{sc} . At the same time, the open-circuit voltage (V_{oc}) of the DSSC decreases monotonically with the ratio of I_2/LiI due to increased dark current in the DSSC. The increased absorption of visible light by the electrolyte, the enhanced dark current, and the reduced ionic conductivity of the electrolyte contribute to the performance variation of the corresponding solid-state DSSC with increasing I_2 concentration.

Introduction

Dye-sensitized solar cells (DSSCs) have been attracting much attention because of their low cost, ease of fabrication, high light-to-electricity conversion efficiencies, and environmentally friendly properties. A light-to-electricity conversion efficiency of more than 11% was achieved in a liquid-electrolyte-based DSSC.^{1–3} To avoid the leakage and evaporation of the organic solvents, many efforts have been made in developing solid or polymer electrolytes.^{4–12} Recently, a series of solid electrolytes based on lithium iodide (LiI) and 3-hydroxypropionitrile (HPN) were found in this group.^{13–15} LiI and HPN can form a compound LiI(HPN)₂ (space group, *C2/c*; $T_m = 142$ °C). It has the feature of monoionic transport of I^- along three-dimensional (3D) diffusion paths in the crystal. LiI(HPN)₄ shows the highest ionic conductivity in this series of solid electrolytes. And a DSSC using LiI(HPN)₄ containing 15% nanosized SiO₂ achieved a high light-to-electricity conversion efficiency of 5.48% under the illumination of 100 mW cm⁻² (AM 1.5).

It is well-known that I_2 exists in the electrolyte containing iodide in the form of polyiodides such as I_3^- or I_5^- (eq 1). An efficient transport of iodide and triiodide in the electrolyte is necessary for good performance of the DSSC because the oxidized state of the dye (dye⁺) should be regenerated by I^- ions efficiently after the electrons from the excited state of the dye are injected into the conduction band of TiO₂ under illumination (eq 2) to reduce the back reactions in the DSSC. Meanwhile, the electrons accumulated at the counter electrode by the external circuit will lead to concentration overpotentials for the electrolyte at the electrode and loss of energy of the

DSSC if the electrons are not transferred by I_3^- efficiently (eq 3).



The introduction of I_2 into liquid or gel electrolytes could increase the conductivity of the electrolyte via a Grotthuss-type charge carrier exchange transfer mechanism.^{16–18} However, the increasing content of I_2 (or I_3^-) leads to enhanced light adsorption even in the visible range by the electrolyte.¹⁹ Therefore, an optimized ratio of I_2/LiI is necessary to achieve better performance of a DSSC. To our knowledge, the influence of the addition of I_2 on the conductivity behavior of the solid electrolyte and the performance of the corresponding DSSC is rarely reported. In this paper, the effects of I_2 addition on the ionic conductivity of the solid electrolyte LiI/HPN = 1:4 (molar ratio) and the performance of the corresponding DSSC are investigated. It is observed that the light-to-electricity conversion efficiency (η) of the DSSC based on the solid-state electrolyte LiI/HPN = 1:4 increases with increasing I_2 concentration until $I_2/LiI = 0.05$. Beyond this value, the η decreases due to the enhancement of dark current in the device, the increase of light absorption by the electrolyte, and the decrease of the ionic conductivity of the solid-state electrolyte LiI/HPN = 1:4.

Experimental Section

Sample Preparation. Anhydrous LiI (99%, Acros Organics) and 3-hydroxypropionitrile (HPN, 98%, Acros Organics) were

* Author to whom correspondence should be addressed. Phone: 86-10-82649242. Fax: 86-10-82649242. E-mail: qbmeng@aphy.iphy.ac.cn

transferred into a glovebox (MBraun) filled with pure argon and used without further treatment. Iodine (I₂, >99.8%, Beijing Yili Organics Company, China) was used as received. Dimethyl carbonate (DMC) and propylene carbonate (PC, battery grade) were employed as solvents. A mixture of LiI, HPN, and I₂ with the required molar ratio was melted and then stirred vigorously to form a homogeneous composite in the glovebox.

Nanocrystalline TiO₂ film was fabricated by a screen-printing technique. The TiO₂ (P25) paste was deposited on a conducting glass substrate (F-doped SnO₂, 10 Ω/□), followed by sintering at 450 °C for 30 min. The thickness of the film was 10 μm. The TiO₂ film was preheated at 120 °C for 30 min before it was immersed into the solution of the dye *cis*-dithiocyanate-*N,N'*-bis(4,4'-dicarboxylate-2,2'-bipyridine) ruthenium(II) (Solaronix) with a concentration of 3×10^{-4} M in dry ethanol overnight. The TiO₂ film covered with the dye was rinsed with dry ethanol before being assembled into a DSSC.

To import the electrolyte into the pores of the TiO₂ film and ensure good wettability of the TiO₂ film with the solid electrolyte, in our experiment, 0.75 g of solid electrolytes with LiI/HPN/I₂ = 1:4:*x* ($0 \leq x \leq 0.1$) were dissolved into 6.0 mL of a cosolvent of DMC + PC (4:1, v/v) in advance. The electrolyte solution was dripped onto the dyed TiO₂ film. Then the solvent was removed under vacuum conditions. Finally, a sandwich-type DSSC configuration was fabricated by holding the thermally platinized indium tin oxide (ITO) counter electrode together with the TiO₂/electrolyte with two clips. The measurements were performed in air. It should be noted that no 4-*tert*-butylpyridine was added into the electrolyte.

Measurements. X-ray diffraction (XRD) data for the electrolytes were collected with a Rigaku B/max-2400 (Cu Kα). Raman spectra of the electrolytes were recorded with a JY-T 64000 Raman spectrometer equipped with a diode laser ($\lambda = 532$ nm) with the power on the sample surface below 5 mW (scan time, 400 s; resolution, 4 cm⁻¹). UV-vis spectra of the electrolytes were detected by a Shimadzu UV-2550. The solid electrolyte was dissolved in PC solvent for this measurement.

Photoenergy conversion efficiency of the DSSC was evaluated by using a solar light simulator (Oriel, 91192) as the light source and a computer-controlled potentiostat (Princeton Applied Research, model 263A). The light intensity at the surface of the cell was modulated by altering the distance between the cell and the simulator to determine the dependence of the short-circuit photocurrent density (*J*_{sc}) of the DSSC on the radiant power (*P*). The intensity of the incident light was measured before each experiment with a radiant power/energy meter (Oriel, 70260). All of the measurements mentioned above were taken at 25 °C.

The ionic conductivity of the solid electrolyte (LiI/HPN/I₂ = 1:4:*x*) was determined with an alternating current (AC) impedance technique on an HP 4192A impedance analyzer from 5 Hz to 13 MHz between 20 and 50 °C. The solid electrolyte was melted before a "stainless steel/electrolyte/stainless steel" type cell was assembled in dry argon. The complex AC impedance spectra were analyzed with the Zview program from Solartron, Inc.

Results and Discussion

X-ray Diffraction Data and Raman Spectra. According to the phase diagram of the binary system LiI/HPN,¹³ the electrolyte becomes solid when the ratio of LiI to HPN is beyond 1:4. The XRD pattern of LiI/HPN = 1:4 at room temperature shows that this pattern contains the phase of LiI(HPN)₂ as shown in Figure 1. Although the microstructure of LiI/HPN = 1:4 is

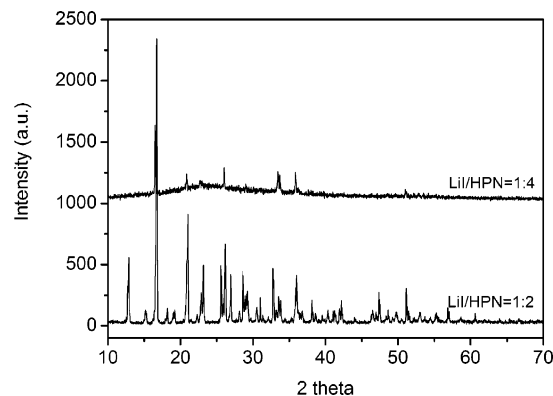


Figure 1. X-ray diffraction pattern of the electrolyte LiI/HPN = 1:4 and LiI/HPN = 1:2 (molar ratio).

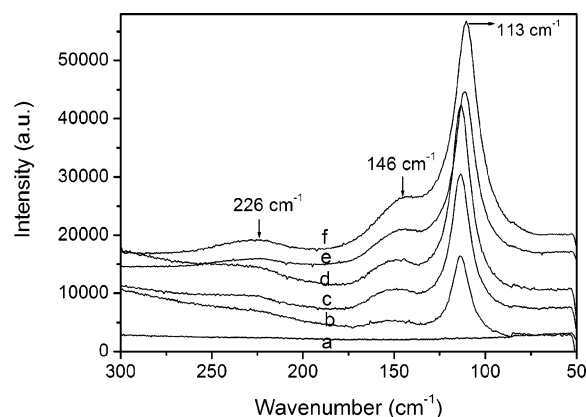


Figure 2. Evolution of Raman spectra of LiI/HPN/I₂ = 1:4:*x* (molar ratio) with changing content of I₂: (a) *x* = 0, (b) *x* = 0.005, (c) *x* = 0.01, (d) *x* = 0.02, (e) *x* = 0.05, (f) *x* = 0.1.

still not clear, it can be supposed that excess 2 mol of HPN in LiI/HPN = 1:4 may exist as the amorphous phase around LiI-(HPN)₂ crystal regions. (See hump background in LiI/HPN (1:4) in Figure 1.)

Figure 2 shows the Raman spectra of LiI/HPN = 1:4 with different ratios of I₂/LiI. No apparent Raman peak can be distinguished between 50 and 300 cm⁻¹ for the electrolyte LiI/HPN = 1:4 before I₂ is added (curve a). The Raman peaks corresponding to the I₃⁻ and I₅⁻ appear even if trace amounts of I₂ are introduced into the electrolyte. For the electrolyte LiI/HPN/I₂ = 1:4:0.005, a band at 113 cm⁻¹ (overtone at 226 cm⁻¹) is assigned to the symmetric stretch of I₃⁻.²⁰ Meanwhile, another band at 146 cm⁻¹ is assigned to the stretch of I₅⁻.²¹ The relative intensities of I₃⁻ and I₅⁻ increase with increasing I₂ concentration. I₃⁻ and I₅⁻ cannot stay in the lattice of the LiI(HPN)₂ crystal due to its space limitation. Therefore, we suppose that I₃⁻ and I₅⁻ may exist at the grain boundaries between the LiI(HPN)₂ phase and the HPN phase after the addition of I₂.

Current-Voltage Characteristics. Figure 3 shows the photocurrent-voltage curve of the DSSC fabricated with the solid electrolyte LiI/HPN/I₂ = 1:4:*x* ($0 \leq x \leq 0.1$). The dependence of *J*_{sc}, *V*_{oc}, the light-to-electricity conversion efficiency (η), and the fill factor (FF) on the I₂ concentration is shown in Figure 4. It is observed that the *J*_{sc} increases from 3.85 to 6.87 mA cm⁻² when the ratio of I₂/LiI (*x*) increases from 0 to 0.05 (Figure 4a). (Here, the ratio value 0 means that no I₂ is added into the electrolyte. The I₃⁻ can be formed due to oxidation of I⁻ by dye⁺ in the operation of the DSSC.¹⁵) Further increasing the I₂ concentration leads to a decrease of the *J*_{sc}. When *x* increases to 0.1, the *J*_{sc} decreases to 5.5 mA

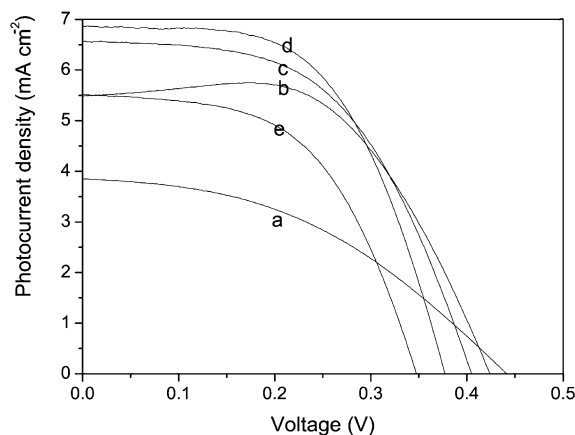


Figure 3. Photocurrent–voltage curve of the DSSC with LiI/HPN/I₂ = 1.4:*x* (molar ratio) employed as the electrolyte: (a) no I₂ added, (b) *x* = 0.01, (c) *x* = 0.02, (d) *x* = 0.05, (e) *x* = 0.1.

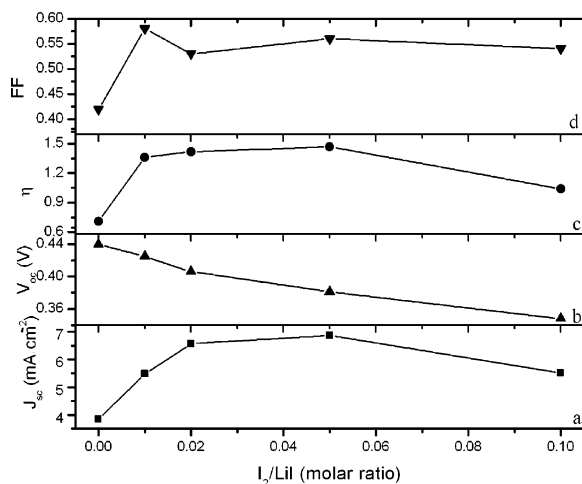


Figure 4. Variation of (a) short-circuit photocurrent density J_{sc} , (b) open-circuit voltage V_{oc} , (c) light-to-electricity conversion efficiency η , and (d) fill factor (FF) with the ratio of I₂/LiI in the electrolyte LiI/HPN = 1.4.

cm^{-2} . In contrast, the V_{oc} decreases gradually with increasing I₂ content in the electrolyte. The FF of the sample with low initial I₂ content is poor due to the severe concentration polarization at the counter electrode.²² With the increase of the I₂ concentration in the electrolyte, the FF increases to a steady value until the ratio of I₂/LiI reaches 0.02 (Figure 4d). A maximum output of 1.5% is obtained from the DSSC fabricated with the solid-state electrolyte LiI/HPN/I₂ = 1.4:0.05 (Figure 4c).

For the DSSC based on the solid electrolyte LiI/HPN = 1:4, the V_{oc} decreases significantly from 0.440 to 0.348 V as the ratio of I₂/LiI increases from 0 to 0.1 (Figure 4b). This can be understood according a theoretical consideration²

$$V_{oc} = (kT/e) \ln(I_{inj}/(n_{cb}k_{et}[I_3^-]))$$

where k is the Boltzmann constant, T is the absolute temperature, e is the electric charge, I_{inj} is the incident photo flux, n_{cb} is the concentration of electrons at the TiO₂ surface, and k_{et} is the rate constant for the back electron reaction.

The photovoltage of a DSSC is kinetically limited by the dark reaction occurring in the photoelectrochemical system (eq 4),^{23,24} where the electrons from the conduction band of TiO₂ recombine with the oxidized species (here, it is I₃[−]) of the redox couple. An increase of the I₂ content leads to an increasing

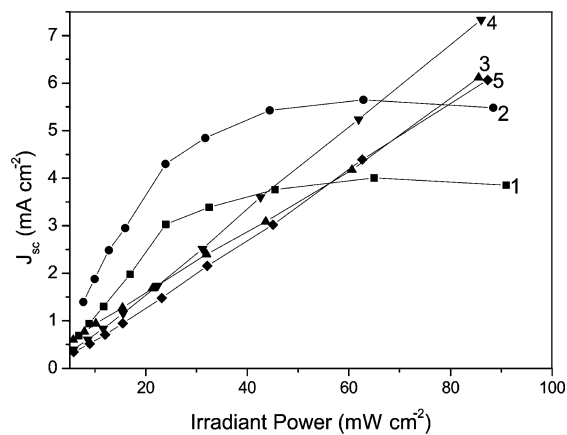
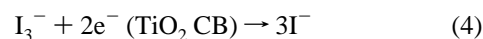


Figure 5. Effect of incident intensity (P) on J_{sc} of a DSSC fabricated with solid-state electrolyte LiI/HPN/I₂ = 1.4:*x* (molar ratio): (1) no I₂ added, (2) *x* = 0.01, (3) *x* = 0.02, (4) *x* = 0.05, (5) *x* = 0.1.

concentration of I₃[−] and an increase of the rate constant for the back electron reaction; thus, the dark current reaction in a DSSC increases. As a result, the V_{oc} decreases.



Besides the electron-transfer/transport rate at the TiO₂ anode of a DSSC, J_{sc} is also determined by two other factors. One is the transport of I[−]/I₃[−] ions in the porous TiO₂ film and in the bulk electrolyte; the other is the electron-transfer process at the counter electrode. In general, when the I₂ content in the electrolyte is very low, the transport of I₃[−] in the porous TiO₂ film and in the electrolyte is very poor, and I₃[−] cannot effectively maintain fast electron transfer at the counter electrodes. Consequently, the J_{sc} of the DSSC appears to saturate with increasing radiation power density. In this situation, J_{sc} is mainly limited by the mass transport of I₃[−] in the electrolyte system.²² Figure 5 shows the effect of the irradiant power on the J_{sc} of a DSSC with LiI/HPN/I₂ = 1.4:*x* (0.01 ≤ *x* ≤ 0.1) as the electrolyte. At low concentrations of I₃[−] (*x* ≤ 0.02), the J_{sc} increases linearly with P at low radiant power ($P < 15 \text{ mW cm}^{-2}$), and it tends to saturate at high radiant power. The lower the initial content of I₂ in the electrolyte, the more the J_{sc} – P relationship deviates from linearity. This indicates that the J_{sc} of the DSSC is limited by the diffusion of I₃[−] in this situation. At high I₃[−] content (*x* ≥ 0.05), the J_{sc} tends to vary linearly with P at both low and high radiant powers, indicating that mass transport does not limit the J_{sc} . Furthermore, it can be seen in Figure 5 that under low radiant power the J_{sc} of the DSSC based on the electrolyte with low I₂ content is higher than that with high I₂ content. This fact indicates that a small amount of I₃[−] is sufficient for supporting fast electron transfer at low radiant power ($P \leq 20 \text{ mW cm}^{-2}$), while the increase of the dark current causes the decrease of the J_{sc} in the case of a high concentration of I₃[−].

A clear understanding of Figure 5 requires the investigation of the transport properties and the adsorption behavior of this electrolyte as shown below.

Ionic Conductivity Investigation. Figure 6 illustrates the Arrhenius plots of the ionic conductivity of the electrolytes LiI/HPN = 1:4 with different I₂ concentrations. Figure 7a shows the dependence of the conductivity of LiI/HPN on the I₂ content at 25 °C. The conductivity of the electrolyte without I₂ is $1.4 \times 10^{-3} \text{ S cm}^{-1}$ at 25 °C. It increases to $1.7 \times 10^{-3} \text{ S cm}^{-1}$ when *x* is 0.01. However, the conductivity decreases gradually when the I₂ content is further increased. At *x* = 0.1, the

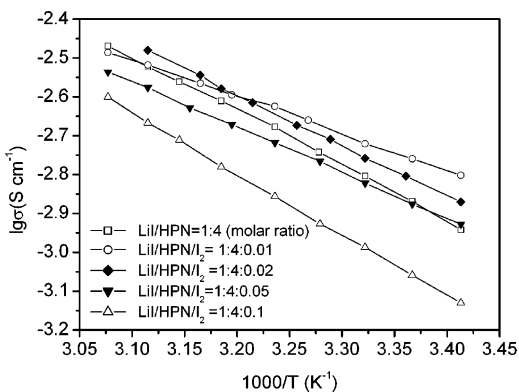


Figure 6. Arrhenius plots of LiI/HPN = 1:4 with different I₂ concentrations.

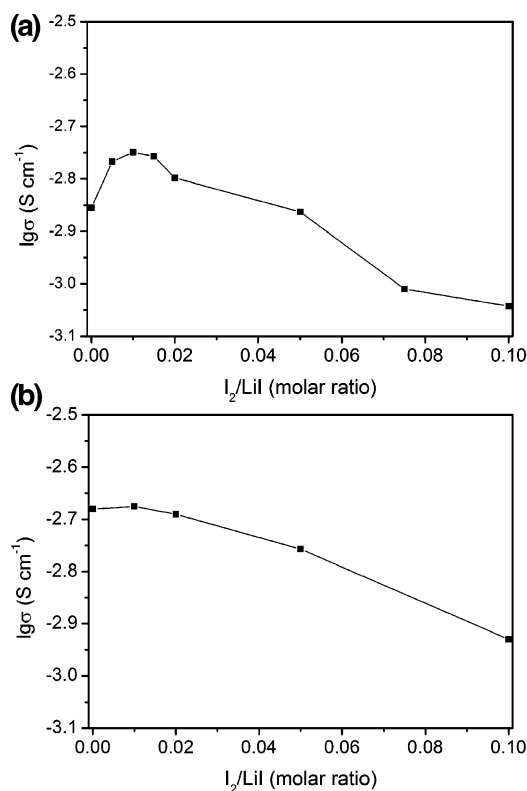


Figure 7. Dependence of the conductivity of the electrolyte (a) LiI/HPN = 1:4 and (b) LiI/HPN = 1:4 with 10 wt % SiO₂ on the I₂ content at 25 °C.

conductivity decreases to $8 \times 10^{-4} \text{ S cm}^{-1}$. This behavior is obviously different from the Grotthus-type charge carrier transfer mechanism, where the ionic conductivity of the electrolyte increases with increasing I₂ concentration in a range of 0–2 M.¹⁸

As mentioned above, I₂ exists in the form of polyiodides (I₃⁻ and I₅⁻) by reaction with I⁻ in the solid electrolyte. The total charge carriers are kept unchanged in the electrolyte system with addition of I₂. It is known that the diffusion coefficients of polyiodides are lower than that of monoiodide due to the larger ionic radius of the former even in liquid electrolyte.¹⁶ It is reasonable that the mobility of I₃⁻ and I₅⁻ is very low in the solid electrolyte. I₃⁻ and I₅⁻ cannot form a continuous bridge for charge transfer as in a liquid system. The ionic conductivity is in proportion to the free ion concentrations and their mobility. The addition of I₂ leads to the increase of the slow charge carriers in the electrolyte. Consequently, the conductivity decreases.

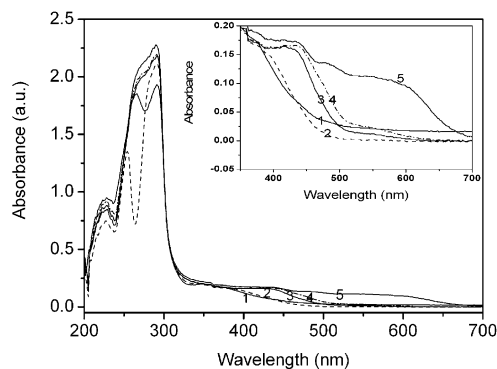


Figure 8. UV-vis spectra of LiI/HPN = 1:4 at different I₂ contents: (1) no I₂ added (solid line), (2) 0.1 mM I₂ (dashed line), (3) 0.5 mM I₂ (solid line), (4) 1.0 mM I₂ (dash-dot line), (5) 25 mM I₂ (solid line).

The slight increase of the ionic conductivity of LiI(HPN)₄ when introducing I₂ into it ($x \leq 0.01$) may come from the decrease of the viscosity of the electrolyte due to the existence of a small amount of HPN in the electrolyte, which leads to the enhancement of the mobility of the ions. However, it is difficult to measure the viscosity of the electrolyte directly because it exists in a solid state. To understand this, a comparison experiment was performed. An electrolyte LiI/HPN = 1:4 containing SiO₂ nanoparticles (15–25 nm, 10 wt %) was prepared. It was observed that the ionic conductivity of the composite electrolyte remained unchanged even at low I₂ content (I₂/LiI $\leq 1:50$; $\sigma = 2.05\text{--}2.1 \times 10^{-3} \text{ S cm}^{-1}$) (Figure 7b). At high I₂ concentrations, the conductivity of the composite electrolyte decreased significantly, consistent with the conduction behavior of LiI/HPN = 1:4. The result indicates that the conduction behavior of the solid electrolyte does not obey the Grotthus mechanism.

UV-Vis Spectra. The absorption of light by the electrolyte LiI/HPN = 1:4 with different I₂ contents was measured by UV-vis spectroscopy (Figure 8). The inset in Figure 8 is the UV-vis spectra of the samples in the range from 350 to 700 nm. The peak at 226 nm belongs to the absorption of I⁻.²⁵ The absorption peak at 253 nm red-shifts and becomes a shoulder of the peak at 292 nm gradually, and its intensity increases with increasing I₂ concentration. This peak should come from the interaction of I⁻ with the PC molecule because a similar absorption peak located at 238 nm was also observed in the KI/PC system (0.3 mM KI in PC). It was observed that two typical absorption peaks of I₃⁻ appear at 363 and 292 nm¹⁹ in LiI/HPN = 1:4 before any addition of I₂ into the electrolyte (curve 1). Their intensities grow with time. A similar phenomenon was also observed in the freshly prepared liquid electrolyte LiI/HPN = 1:10 (not shown). However, no absorption peak of I₃⁻ was observed in the freshly prepared LiI/PC solution. Therefore, the formation of I₃⁻ in the LiI/HPN system without the addition of I₂ should result from an interaction between I⁻ and the HPN molecule. It was reported that I⁻ tended to become I₃⁻ in the solution of *tert*-butyl alcohol or pyridine.²⁵ The reason was not explained there. We suppose here that I⁻ is oxidized by HPN in our system. The detailed reaction mechanism requires further clarification.

The relative intensity of the absorption peak at 292 nm in the spectrum increases with increasing I₂ concentration. Addition of a small amount of I₂ leads to a red-shifting of the peak at 363 nm. When the concentration of I₂ in the LiI(HPN)₄/PC solution reaches 25 mM, the absorption of light by the electrolyte solution extends even beyond 600 nm (curve 5). A similar phenomenon has been reported in other systems.^{18,26} However,

this part of the absorption does not contribute to the net output current of the DSSC. Meanwhile, the increase of the I_3^- concentration in the electrolyte results in an increasing dark current of the DSSC.²⁶ The dark current influences the V_{oc} of the DSSC as discussed above. Due to the decrease of the ionic conductivity of the electrolyte and the increase of the absorption of the electrolyte of visible light with increasing I_2 concentration, J_{sc} of the DSSC decreases when I_2 content is beyond a limitation. Considering the dependence of J_{sc} and V_{oc} on the I_2 content as discussed above, a maximum light-to-electricity conversion efficiency of 1.5% was achieved for an $LiI/HPN/I_2 = 1:4:0.05$ solid-state DSSC.

Conclusions

The ionic conductivity of the solid-state electrolyte $LiI/HPN = 1:4$ decreases dramatically with increasing I_2 concentration. The low mobility of polyiodides such as I_3^- and I_5^- contributes to the variation of the ionic conductivity of the electrolyte after I_2 is added. The open-circuit photovoltage (V_{oc}) of the DSSC assembled with $LiI/HPN/I_2 = 1:4:x$ (molar ratio) decreases monotonically with increasing I_2 content due to the increase of the dark current in the device. The short-circuit photocurrent density (J_{sc}) of the corresponding DSSC initially increases, then begins to decrease with increasing I_2 concentration. J_{sc} is affected by several factors. At low I_2 (I_3^-) content, the J_{sc} is mainly controlled by the diffusion of I_3^- in the DSSC. Increasing I_2 content leads to an increase of J_{sc} . However, the ionic conductivity of the electrolyte, the absorption of visible light by the electrolyte, and the dark reaction in the DSSC also increase with increasing I_2 concentration, which reduces the J_{sc} . As a result of the above factors, a maximum J_{sc} is achieved at $I_2/LiI = 0.05$. A 1.5% of light-to-electricity conversion efficiency of the solid-state DSSC is obtained at the optimum ratio of $LiI/HPN/I_2 = 1:4:0.05$ under the radiation of 100 mW cm^{-2} (AM 1.5).

Acknowledgment. The authors appreciate the financial support from the National 863 Program of China (Contract No. 2002AA302403), the National 973 Program, and the "100-Talent" project of Chinese Academy of Sciences.

References and Notes

- O'Regan, B.; Grätzel, M. *Nature* **1991**, *335*, 737.
- Nazeeruddin, M. K.; Kay, A.; Rodicio, I.; Humphry, R.; Muller, E.; Liska, P.; Vlachopoulos, N.; Grätzel, M. *J. Am. Chem. Soc.* **1993**, *115*, 6382.
- Grätzel, M. *Inorg. Chem.* **2005**, *44*, 6841.
- O'Regan, B.; Schwartz, D. T. *Chem. Mater.* **1995**, *7*, 1349.
- Tennakone, K.; Fernando, C. A. N.; Dewasurendra, M. J. *J. Photochem.* **1987**, *38*, 75.
- Meng, Q.-B.; Takahashi, K.; Zhang, X.-T.; Sutanto, I.; Rao, T. N.; Sato, O.; Fujishima, A. *Langmuir* **2003**, *19*, 3572.
- Wang, P.; Zakeeruddin, S. M.; Moser, J.-E.; Grätzel, M. *J. Phys. Chem. B* **2003**, *107*, 13280.
- Cao, F.; Oskam, G.; Searson, P. C. *J. Phys. Chem.* **1995**, *99*, 17071.
- Wang, P.; Dai, Q.; Zakeeruddin, S. M.; Forsyth, M.; MacFarlane, D. R.; Grätzel, M. *J. Am. Chem. Soc.* **2004**, *126*, 13590.
- Dai, Q.; MacFarlane, D. R.; Howlett, P. C.; Forsyth, M. *Angew. Chem., Int. Ed.* **2005**, *44*, 313.
- Bach, U.; Lupo, D.; Comte, P.; Moser, J. E.; Weissortel, F.; Salbeck, J.; Spreitzer, H.; Grätzel, M. *Nature* **1998**, *395*, 583.
- Gazotti, W. A.; Giroto, E. M.; Nogueira, A. F.; De Paoli, M.-A. *Sol. Energy Mater. Sol. Cells* **2001**, *69*, 315.
- Wang, H. X.; Xue, B. F.; Hu, Y. S.; Wang, Z. X.; Meng, Q. B.; Huang, X. J.; Chen, L. Q. *Electrochem. Solid-State Lett.* **2004**, *7*, A302.
- Wang, H.; Wang, Z.; Xue, B.; Meng, Q.; Huang, X.; Chen, L. *Chem. Commun.* **2004**, 2186.
- Wang, H.; Li, H.; Xue, B.; Wang, Z.; Meng, Q.; Chen, L. *J. Am. Chem. Soc.* **2005**, *127*, 6394.
- Papageorgiou, N. *Coord. Chem. Rev.* **2004**, *248*, 1421.
- Kubo, W.; Murakoshi, K.; Kitamura, T.; Yoshida, S.; Haruki, M.; Hanabusa, K.; Shirai, H.; Wada, Y.; Yanajida, S. *J. Phys. Chem. B* **2001**, *105*, 12809.
- Kubo, W.; Kambe, S.; Nakade, S.; Kitamura, T.; Hanabusa, K.; Wada, Y.; Yanagida, S. *J. Phys. Chem. B* **2003**, *107*, 4374.
- Popov, A.; Swemsem, R. F. *J. Am. Chem. Soc.* **1955**, *77*, 3724.
- Andrews, L.; Prochaska, E. S.; Loewenschuss, A. *Inorg. Chem.* **1980**, *19*, 463.
- Tadayoni, M. A.; Gao, P.; Weaver, M. J. *J. Electroanal. Chem.* **1986**, *198*, 125.
- Huang, S. Y.; Schlichthorl, G.; Nozik, A. J.; Grätzel, M.; Frank, A. J. *J. Phys. Chem. B* **1997**, *101*, 2576.
- Liu, Y.; Hagfeldt, A.; Xiao, X.; Lindquist, S.-E. *Sol. Energy Mater. Sol. Cells* **1998**, *55*, 267.
- Rosenblut, M. L.; Lewis, N. S. *J. Phys. Chem.* **1989**, *93*, 3735.
- Kebede, Z.; Lindquist, S.-E. *Sol. Energy Mater. Sol. Cells* **1999**, *57*, 259.
- Papageorgiou, N.; Athanassov, Y.; Kitamura, T.; Armand, M.; Bonhote, P.; Pettersson, H.; Azam, A.; Grätzel, M. *J. Electrochem. Soc.* **1996**, *143*, 3099.